Two-Dimensional ^{1}H NMR of Gene 5 Protein Indicates That Only Two Aromatic Rings Interact Significantly with Oligodeoxynucleotide Bases†

Garry C. King and Joseph E. Coleman*
Department of Molecular Biophysics and Biochemistry, Yale University, New Haven, Connecticut 06510
Received June 5, 1986; Revised Manuscript Received December 9, 1986

ABSTRACT: The interaction of gene 5 protein (G5P) with oligodeoxynucleotides is investigated by ^{1}H NMR methods, principally two-dimensional nuclear Overhauser effect spectroscopy (NOESY). Aromatic resonances of G5P are specifically assigned from crystallographic data, while the low-field resonances of nucleotides are assigned with sequential or other procedures. Chemical shift changes that accompany binding of $d(pA)_4$, $d(A)_4$, $d(pT)_4$, and $d(pA)_8$, combined with specific protein–nucleotide nuclear Overhauser effects (NOEs) obtained from NOESY spectra, suggest that Phe-73 and Tyr-26 are the only aromatic residues that stack significantly with nucleotide bases. Chemical shift data also imply a role for Leu-28, though this has not been confirmed with intermolecular NOEs. Binding of all four oligonucleotides causes marked upfield movements (0.1–0.6 ppm) of G5P NOESY cross peaks belonging to Tyr-26, Leu-28, and Phe-73. Most other G5P spin systems, notably those of Tyr-34 and Tyr-41, do not appear to be significantly affected. In the $d(pA)_4$–G5P complex an intermolecular NOE is observed between Tyr-26 and H1′ of Ade-1, while Phe-73 has NOEs with the H2, H8, and H1′ protons of Ade-2 and -3. Intermolecular NOEs seem to follow a similar pattern in the partially cooperative $d(pA)_8$–G5P complex, though specific nucleotide resonance assignments are not possible in this case. Binding causes relatively small chemical shift changes for the base resonances in adenylyl nucleotides, suggesting that there is some, but not complete, unstacking of the bases. In the $d(pA)_8$ complex, the upfield ring current shifts of the Tyr-26 and Phe-73 resonances become greater than those caused by $d(pA)_4$, implying that cooperative interactions result in a tighter complex. The view of the G5P–oligonucleotide interaction that emerges from this study is different from one previously proposed from model-building exercises [Brayer, G. D., & McPherson, A. (1984) *Biochemistry 23*, 340–349]. The major point of difference concerns the role of Tyr-41, which has been postulated to stack with nucleotide bases. Our NMR data provide no support for this proposal. Rather, a comparison of the NMR data with the X-ray structure of native G5P suggests that Tyr-26, Leu-28, and Phe-73′ form the major components of a dominant nucleotide interaction site that lies near a phosphate-binding electropositive cluster formed by the side chains of Arg-16, Arg-21, Lys-24, and Lys-46. Such an interaction mode creates a shorter nucleotide path across the protein surface than previously proposed. At present it is unclear whether a shorter nucleotide path is relevant to the much larger G5P–fd DNA complex, but it may facilitate "inside" packing of DNA in the macromolecular superhelix, reconciling previous neutron-scattering data with a structural model.

Gene 5 protein (G5P)[1] acts to regulate DNA synthesis in the life cycle of the fd (M13) bacteriophages by complexing with single-stranded progeny DNA [Alberts et al., 1972; for a review see Kornberg (1980, 1982)]. Since G5P can be viewed as a prototypical single-stranded binding protein (Coleman & Oakley, 1980), there has been a particular interest in elucidating the molecular features that confer its preference for single-stranded DNA.

The functional species of G5P is a stable dimer (Pretorius et al., 1975; Cavalieri et al., 1976; Pörschke & Rauh, 1983), constituted by identical monomers of 87 residues (Nakashima et al., 1974; Cuypers et al., 1974). It is the only single-strand binding protein whose X-ray crystal structure is known at present (Brayer & McPherson, 1983). A refined model of the native protein at 2.3-Å resolution reveals that the two monomers are intimately associated about a dyad axis, a symmetry that places two putative DNA binding channels in an antiparallel orientation on one face of the dimer (Brayer & McPherson, 1983). These channels each contain exposed Arg, Lys, Tyr, and Phe residues, amino acids shown by earlier physicochemical studies to be involved in the G5P–ssDNA interaction (Anderson et al., 1975; Coleman et al., 1976; Garssen et al., 1977; Coleman & Armitage, 1978; Alma et al., 1981a).

As yet, attempts at direct crystallographic visualization of the protein–DNA interaction have not been successful, though high-quality G5P–$d(pA)_4$ crystals were reported recently (McPherson et al., 1986). In the absence of a cocrystal structure, Brayer and McPherson have used molecular-modeling procedures to generate a plausible description of the protein–DNA complex (Brayer & McPherson, 1984; McPherson & Brayer, 1985). Their proposed model places a chain of five nucleotides, in fully extended conformation, along a DNA binding channel that extends from Tyr-26 to Tyr-41 in a 5′ to 3′ direction. The phosphate backbone is bound by four basic residues, two from the "DNA binding loop" (a protruding peptide loop composed of residues 15–32) and two from the main body of the protein, while each nucleotide base is stacked against an aromatic side chain. A postulated structure for the native G5P–fd DNA superhelix has been generated by extension of this model through atomic

† This work was supported by Grant GM 21919-11 from the National Institutes of Health.

[1] Abbreviations: COSY, 2D scalar correlated spectroscopy; CPA, Carr–Purcell method A; CPMG, Carr–Purcell–Meiboom–Gill; dTyr, perdeuteriotyrosine; G5P, gene 5 protein; NOE, nuclear Overhauser effect; NOESY, 2D nuclear Overhauser effect spectroscopy; TNM, tetranitromethane; 2D, two dimensional; 1D, one dimensional.

0006-2960/87/0426-2929$01.50/0

contact analysis (Brayer & McPherson, 1985; McPherson & Brayer, 1985). Though consistent with a reasonable portion of the available physicochemical data, the Brayer–McPherson model is at variance with several findings for G5P–fd DNA and G5P–homopolymer complexes. At a fundamental level, the chosen stoichiometry of five nucleotides per monomer differs from the stoichiometry of four nucleotides per monomer that dominates the literature (Alberts et al., 1972; Oey & Knippers, 1972; Day, 1973; Anderson et al., 1975; Cavalieri et al., 1976; Coleman et al., 1976; Alma et al., 1983a; Pörschke & Rauh, 1983). Their model of the G5P–fd DNA complex also places the DNA on the "outside" of the nucleoprotein superhelix, in apparent disaggreement with neutron-scattering data which indicates that the DNA has a smaller radius of gyration than the protein (Gray, D. M., et al., 1982).

In view of these problems, we feel that further experimental examination is required in order to probe the solution behavior and interactions of G5P. NMR spectroscopy, which has been usefully applied to G5P in the past (Coleman et al., 1976; Garssen et al., 1977, 1978, 1980; Coleman & Armitage, 1977, 1978; Hilbers et al., 1978; Alma et al., 1981a,b, 1982, 1983b; O'Connor & Coleman, 1982, 1983), can be used to test for specific molecular interactions predicted by models of G5P–nucleotide complexes. This paper describes the application of 2D NOESY spectra to an investigation of the interaction between G5P and short oligodeoxynucleotides.

Materials and Methods

Gene 5 Protein and Oligodeoxynucleotides. G5P was prepared by a previously described method (Anderson et al., 1975), as was protein containing perdeuteriotyrosine (dTyr–G5P) (Coleman & Armitage, 1978). The protein monomer concentration was determined spectrophotometrically from ϵ_{276} = 7100 M^{-1} cm^{-1} (Day, 1973), and all quoted concentrations refer to the monomer species. The nucleotides $d(pA)_4$, $d(A)_4$, $d(pA)_8$, and $d(pT)_4$ were purchased from Pharmacia P-L Biochemicals and used without further purification. Concentrations were determined from data supplied by the manufacturer and refer to the oligonucleotide species rather than to nucleotide monomers.

NMR Spectroscopy. Protein and oligodeoxynucleotide solutions for NMR were prepared by multiple lyophilizations from deuteriated buffer or by solvent exchange on a Sephadex G-25 spun column. Working G5P monomer concentrations were in the range 1.0–1.8 mM, close to the maximum solubility obtainable under normal conditions. Samples were routinely run at 25–35 °C. At the upper end of this temperature range, line width improvements were significant, but some irreversible coating of G5P onto the NMR tube frequently occurred. The presence of this coating was not found to cause significant spectral changes.

NMR spectra were recorded on the Bruker 490-MHz and WM-500 spectrometers at the Yale University Chemical Instrument Center. Absolute value COSY spectra were acquired with standard methods. Pure absorption NOESY spectra were acquired with the method of States et al. (1982). Typical NOESY data sets contained 125–256 t_1 experiments, with 256–512 total scans per experiment. A relaxation delay of 1.0 s was routine, leading to total experimental times of 24–36 h. 2D data were transferred to a Vax 11/750 computer for processing with the FTNMR software of Dr. D. Hare (copyright). Skewed phase-shifted sine-bell functions were used for spectral optimization. Unless otherwise stated, NOESY spectra were routinely subjected to the t_1 noise reduction procedure of Klevit (1985), followed by symmetrization (Baumann et al., 1981).

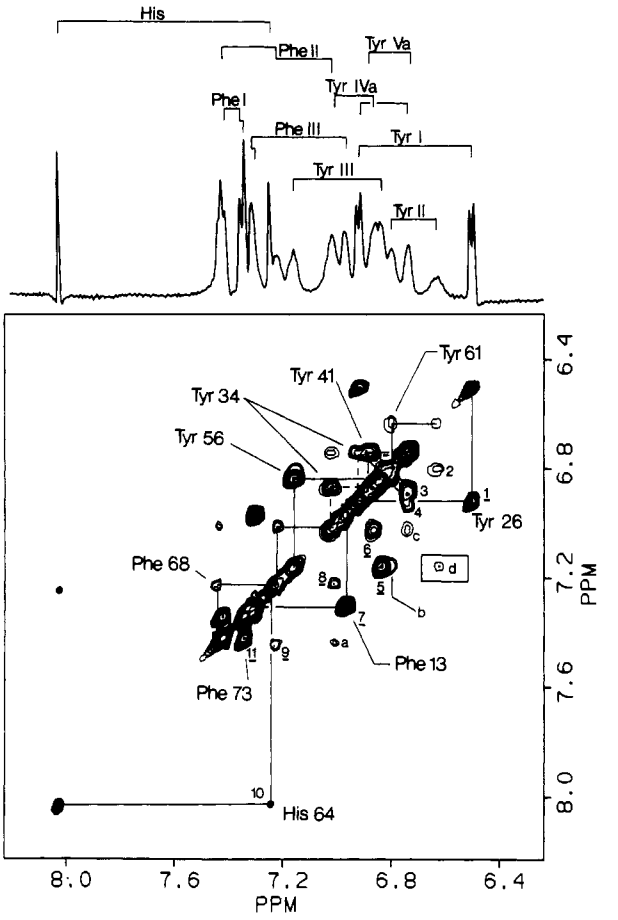

FIGURE 1: Aromatic region from a 200-ms NOESY spectrum of native G5P, with 1D reference spectrum and assignments determined in this work (conditions: 1.5 mM G5P in 25 mM phosphate, pH 7.6, 35 °C). Nearest-neighbor NOESY correlations are numbered 1–11, where the underlined cross peaks reflect positions at which connectivities have been observed in COSY spectra. Longer range correlations are designated a–d; peak d (inset) is contoured at a lower level. Nonspecific assignments follow the nomenclature of Alma et al. (1981b), with amendments designated by the suffix a.

Structural Calculations. Crystal coordinates for the G5P monomer were obtained from the Protein Data Bank. In order to add H-bonding groups, improve the geometric ideality, and remove unfavorable contacts that appeared to be present on examination of the structure, the dimer coordinates were generated and subjected to 1000 cycles of energy minimization with the program AMBER (Weiner et al., 1984). A united atom force field, distance-dependent dielectric, and nonbonded cutoff of 8 Å were used. The root mean square movement of all atoms after this procedure was 1.1 Å, relatively evenly distributed throughout the structure. An approximate G5P–DNA model was constructed from the energy-reduced protein structure and $d(pA)_4$ in the B conformation, with an Evans and Sutherland picture graphics system and FRODO (Jones, 1978).

Results and Discussion

G5P Resonance Assignments. Sequence-specific assignment of the G5P aromatic resonances is desirable before a detailed description of the protein–nucleotide interaction is attempted. Assignments determined in this work are summarized in Figures 1 and 2 and Table I. The spectral regions shown in Figures 1 and 2 are very much best examples with our present instrumentation; other regions from NOESY spectra of G5P have a much poorer appearance. This and the poor quality of the COSY spectra that we have obtained to date suggest

Table I: Resonance Assignments for Native G5P in 25 mM Phosphate, pH 7.6, 35 °C

resonance[a]		δ_{obsd}	resonance[a]		δ_{obsd}
His-64	C-2 H	8.03	Phe-73 (I)	(2,6)H	7.42
	C-4 H	7.24		(3,5)H	7.35
Val-4?	γ_1-CH_3	1.10		(4)H	7.35
Val-35?	CH_3	1.25	Tyr-26 (I)	(2,6)H	6.91
Leu-28	δ-CH_3	0.88		(3,5)H	6.50
		0.93	Tyr-34 (IVa)	(2)H	7.03
Leu-83	δ_1-CH_3	0.37		(3)H	6.87
	δ_2-CH_3	−0.52		(5)H	6.91
Phe-13 (III)	(2,6)H	6.97		(6)H	6.75
	(3.5)H	7.31	Tyr-41 (Va)	(2,6)H	6.89
	(4)H	7.31		(3,5)H	6.74
Phe-68 (II)	(2,6)H	7.44	Tyr-56 (III)	(2,6)H	7.16
	(3.5)H	7.23		(3,5)H	6.84
	(4)H	7.02	Tyr-61 (II)[b]	(2,6)H	6.64
				(3,5)H	6.81

[a] Nonspecific designations for the aromatic spin systems (Alma et al., 1981b) appear in parentheses. The suffix "a" denotes an amendment made in this work. [b] (2,6)H is upfield of (3,5)H as determined by selective deuteriation.

that sequential assignment procedures will be of limited utility for this protein.

The first step in the assignment process, identification of individual spin systems, has been previously reported by Alma et al. (1981b). Since most (though not all) of our nonspecific assignments are in agreement with these authors', we will base our description of individual spin systems on their Roman numeral convention. A 200-ms NOESY spectrum of native G5P (Figure 1) contains most of the information necessary for nonspecific assignment of the nine aromatic spin systems. Eleven of these NOESY correlations (cross peaks 1–11) can be observed in spectra acquired at 100-ms mixing time, indicating that they derive from intraresidue nearest-neighbor connectivities. This information would normally be obtained from COSY spectra, but the relatively large line widths of some G5P resonances prevent them from manifesting COSY cross peaks of significant intensity. However, seven aromatic cross peaks have been observed in COSY spectra to date, each of which is consistent with the NOESY data. The nonspecific assignment scheme shown with the 1D reference spectrum of Figure 1 has been made after examination of the spectrum of dTyr–G5P (not shown) and allocation of the corresponding NOESY cross peaks to phenylalanine groups. Phenylalanine spin systems identified by selective deuteriation are in perfect agreement with earlier proposals (Alma et al., 1981b).

The specific assignment procedure used here relies on crystallographic and to a lesser extent chemical modification data. The basic strategy hinges on the presence of a relatively small number of aromatic residues, each occupying a spectroscopically unique site. Assignment of the whole set of aromatic resonances in a self-consistent manner lends an extra measure of determinancy that is not present when only a fraction of the resonances is assigned. A somewhat more extensive version of this approach has been recently applied to plastocyanin (King & Wright, 1986). Evidence used in the assignment process is presented according to residue type, with incidental methyl group assignments where they can be made with a reasonable degree of certainty.

(*A*) *Histidine.* Two singlet resonances at 8.03 and 7.24 ppm have been assigned to the C-2 H and C-4 H groups of the sole histidine, His-64 (Alma et al., 1981b). We assume that the usual chemical shift order of these resonances (Bundi & Wüthrich, 1979) is retained in the salt-bridged or H-bonded environment indicated by the X-ray structure (Brayer & McPherson, 1983). At 200-ms mixing time, an NOE of approximately 4% intensity is observed between the C-2 H and C-4 H resonances (peak 10 in Figure 1), representing an interproton distance of 4.2 Å that is fixed by imidazole ring geometry. The presence of this NOE is not unreasonable given the molecular weight of G5P and the 200-ms mixing time employed. Both ring proton resonances are involved in NOEs with a methyl group signal at 1.10 ppm (Figure 2) expected to derive from the nearby Val-4 γ_1-CH_3 group.

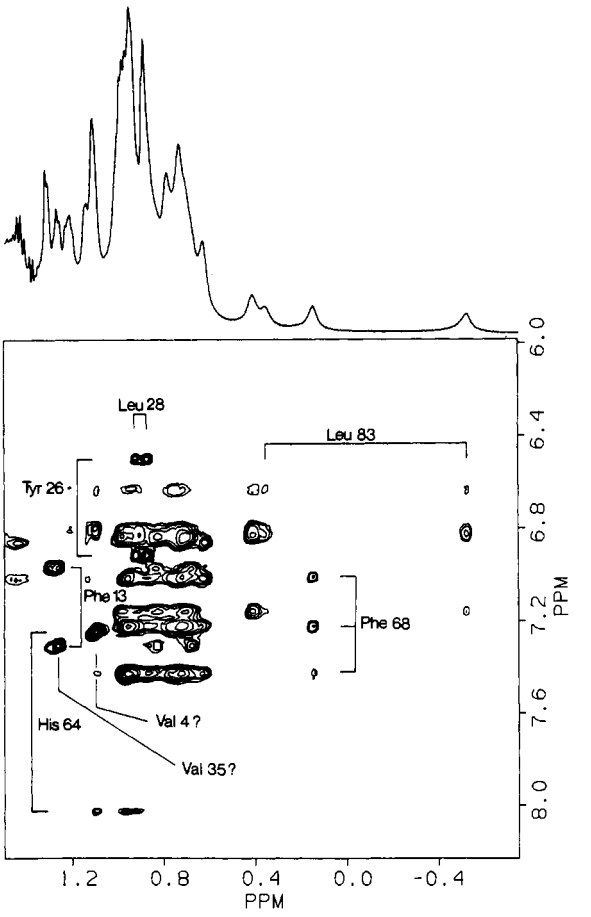

FIGURE 2: Aromatic-to-methyl correlations from the spectrum of Figure 1. Selected sequence-specific resonance assignments are indicated.

(*B*) *Phenylalanine.* Each of the phenylalanine spin systems (Figure 1) is as proposed by Alma et al. (1981b). The Phe I spin system has the sharpest resonances in the aromatic region [as indicated by CPMG spectra (Campbell et al., 1975)], exhibits chemical shifts close to the random coil values (Perkins, 1980), and shows no discernible NOEs with methyl group signals. Such behavior is expected only for the resonances of Phe-73, the unique phenylalanine residue that occupies a fully exposed position in the X-ray structure. The second Phe spin system exhibits a resolved (2,6)H–(4)H NOE at a mixing time of 200 ms (peak a in Figure 1), reflecting an interproton distance of 4.2 Å. This spin system has well-dispersed resonances unlike the other two phenylalanines and is assigned to Phe-68, which lies buried near the dyad axis within the ring current fields of His-64 and its symmetry-related partner Phe-68′.[2] Consistent with the buried position

[2] The superscript prime notation refers to a residue that derives from the second G5P monomer and is used in cases where monomer-specific spatial information is necessary for clarity. Thus, Tyr-26 and Phe-73′ are the relevant aromatics that contribute to a single binding cleft. Some residues at the monomer–monomer interface may also come into proximity with their own symmetry-related counterparts. NMR spectra are generally not considered in a monomer-specific manner since there is no evidence for spectral inequivalence.

of Phe-68, its resonances exhibit NOEs with several methyl group signals, including those at 0.16, 0.73, 0.87 and 0.96 ppm (Figure 2). The X-ray structure predicts that methyl groups of Val-63, Val-4, and Met-77 lie within 4.0 Å of Phe-68 protons, while more lie within 6 Å. The remaining phenylalanine spin system is assigned to Phe-13 by elimination. In accord with this proposal, its resonances are involved in a single intense NOE with a methyl group signal (Figure 2), expected to derive from Val-35, the sole methyl-containing residue that lies within 5.0 Å.

(*C*) *Tyrosine.* The five tyrosine spin systems give rise to six distinct nearest-neighbor connectivities (peaks 1–6 in Figure 1), indicating that one spin system possesses the ABCD pattern characteristic of an immobilized residue or that a slow chemical exchange process is present. Three AA′XX′ spin systems can be identified unequivocally. The Tyr II and Tyr III systems exhibit interresidue NOEs (peaks b and d in Figure 1) that identify them as the unique Tyr-56–Tyr-61 pair (Brayer & McPherson, 1983), whose protons approach as close as 2.6 Å from each other in the X-ray structure. The interresidue NOEs are quite intense but appear less so in contour plots due to the large line widths of the Tyr II resonances. Chemical modification studies (Anderson et al., 1975) indicate that Tyr-56 readily reacts with TNM while Tyr-61 does not, leading us to assign the Tyr III system to Tyr-56 on the basis that its sharper lines are consistent with a more exposed location. Resonances from both residues show NOEs with several methyl signals, including the ring current shifted resonances at 0.41, 0.37, and −0.52 ppm. According to the crystal structure, protons from the methyl groups of Leu-49, Ile-47, and Leu-83 lie within 4.0 Å of Tyr-56 protons, while Tyr-61 is closest to Leu-83. The presence of an NOE between the methyl resonances at 0.37 and −0.52 ppm and the results of ring current shift calculations (data not shown) allow tentative assignment of these signals to Leu-83. Resonances from the Tyr I spin system are unusually sharp and can be identified from the fact that they and the Phe I resonances shift in a correlated manner when a mononucleotide binds to a unique site on the protein surface (O'Connor & Coleman, 1983). This behavior is only possible for Tyr-26 and Phe-73′,[2] since the other tyrosines are either too distant from the exposed phenylalanine or too inaccessible. The Tyr-26 resonances are involved in NOEs with two unusually sharp methyl signals at 0.93 and 0.88 ppm assigned to Leu-28 (Figure 2), which lies on the DNA binding loop near Tyr-26. In passing, we note that relative line width/mobility arguments become more compelling as protein size increases.

Both remaining tyrosine spin systems are clearly defined by cross peaks 3, 4, and 6 in Figure 1 and differ from the nonspecific assignments of Alma et al. (1981b). The Tyr IVa system can be interpreted in terms of an ABCD pattern with a transannular NOE between its (2)H and (6)H resonances (peak c in Figure 1). Resonance overlap would prevent the observation of a similar NOE between the (3)H and (5)H resonances. Proton counting in the 1D spectrum suggests that the (2)H signal does have the expected one-proton intensity. Since the contacts responsible for the apparent immobilization of this ring may also make it inaccessible to TNM, the Tyr IVa spin system is assigned to Tyr-34, which is not susceptible to chemical modification (Anderson et al., 1975). The Tyr Va spin system (peak 3 in Figure 1) is assigned to Tyr-41 by elimination.

Sequence-specific NMR assignments based on crystallographic data should always be treated with a degree of caution, since experience has shown that errors are possible when a system is not considerably overdetermined. This is particularly so given the somewhat troubled history of the G5P X-ray structure (Brayer & McPherson, 1983; McPherson et al., 1979). Given the spectroscopic difficulties of the G5P system, the internal consistency of the proposed assignments gives some confidence in their essential correctness, though the Tyr-34 and Tyr-41 assignments are not as firmly distinguished as the rest. In particular, those assignments critical to the rest of this work (Tyr-26 and Phe-73) have the greatest certainty. Even if the Tyr-56, Tyr-61, Tyr-34, and Tyr-41 assignments presented here were to be totally wrong, the broad conclusions drawn from our nucleotide binding experiments would be unaffected. In time, we expect that direct tests of these assignments, such as the site-directed mutagenesis approach of Prigodich et al. (1986) will be undertaken. Meanwhile, we feel that there is sufficient experimental justification for them to be used as a working set.

Structural Inferences from Assignment Process. Though our NMR data are somewhat limited in nature, they do provide some useful information on the microenvironments of the aromatic residues. The DNA binding loop is a region of the protein that has been proposed to have functional importance (Brayer & McPherson, 1983). In the crystal, this loop contacts protein in the next unit cell, with the consequent possibility that its excursion from the main body of the body of the protein is a result of crystal-packing requirements. The apparent absence of NOEs from Tyr-26 and Leu-28 onto Phe-73, in concert with the unusual sharpness of the Tyr-26 and Leu-28 resonances, suggests that the loop does adopt a similar conformation in solution. Resonances from Phe-73 are also unusually sharp, suggesting that this ring is extended toward the solvent in a manner that would assist in its interaction with nucleic acid bases.

There is some indication of environmental differences between crystal and solution in the vicinity of the monomer–monomer interface. Though the X-ray structure predicts that Val-4 is very close to both His-64 and Phe-68, the methyl signal involved in a large NOE with the His-64 C-4 H resonance (Figure 2) has no significant NOE with the Phe-68 resonances. Both the His-64 and Phe-68 assignments are very firm, so this observation cannot arise from an assignment error. Simiarly, a large NOE is expected between the Phe-68 ring and the ε-methyl group of Met-77, but neither of the Met methyl resonances (which can be readily identified from CPA spectra) show significant NOEs onto any aromatic signal. Again, the presence of an assignment error would have resulted in an unexpected NOE from the Met methyl resonances, but no such NOEs are observed. These observations could probably be accommodated by relative atomic movements of 2 Å or less and may reflect the fact that crystallographic refinement was performed on the monomer (which constitutes the asymmetric unit) rather than on the dimer (Brayer & McPherson, 1983). With the exception of the above considerations, our data so far suggest that the solution and crystal structures are very similar.

Complexation of G5P with $d(pA)_4$ and $d(A)_4$. NOESY spectra have the potential to provide detailed information on the complexation of G5P with short oligonucleotides. To allow direct comparison with earlier 1D NMR studies, this potential has been initially probed in experiments involving adenine-containing deoxynucleotides, which adopt an average conformation similar to one strand of B-DNA (Oltshoorn et al., 1980). As expected from previous reports (Coleman & Armitage, 1978; O'Connor & Coleman, 1983), we observe that addition of excess $d(pA)_4$ to G5P causes specific changes in

Table II: Chemical Shift Changes Resulting from Complexation of G5P with Oligonucleotides[a]

resonance		Δδ (ppm)[b]			
		$d(pA)_4$	$d(A)_4$	$d(pA)_8$	$d(pT)_4$
Phe-13	(2,6)H	−0.03[c]	−0.02[c]	−0.04	−0.04
	(3,5)/(4)H	−0.01	0.00	−0.02	−0.01
Leu-28	δ-CH_3	−0.13	−0.14	−0.18	−0.09
		−0.14	−0.13	−0.18	−0.10
Tyr-26	(2,6)H	−0.14	−0.11	−0.18	−0.08
	(3,5)H	−0.19	−0.13	−0.23	−0.12
Tyr-34	(2)H	0.00	0.00	0.00	0.00
	(3)H	0.00	0.00	0.00	0.00
	(5)H	0.00	0.00	0.00	0.00
	(6)H	−0.06	0.00	−0.07	−0.04
Tyr-41	(2,6)H	−0.04	0.00		
	(3,5)H	0.04	0.00		
Phe-73	(2,6)H	−0.27	−0.22	−0.55	−0.15
	(3,5)/(4)H	−0.28	−0.22	−0.50	−0.15
Ade-1	H8	−0.08[d]	−0.05		
	H2	0.03	−0.01		
	H1′	−0.07	−0.06		
Ade-2	H8	−0.03	−0.02		
	H2	0.13	0.05		
	H1′	0.08	0.01		
Ade-3	H8	−0.02	−0.04		
	H2	0.14	0.03		
	H1′	0.04	0.01		
Ade-4	H8	−0.06	−0.02		
	H2	0.02	0.01		
	H1′	−0.07	−0.02		

[a] Conditions: 10 mM phosphate, 100 mM NaCl, pH 7.6, 35 °C. [b] Estimated error ±0.01 ppm. [c] Protein resonance shifts caused by 1.5:1 $d(pA)_4$, 1.1:1 $d(A)_4$, 0.5:1 $d(pA)_8$, or 1.1:1 $d(pT)_4$. [d] Nucleotide resonance shifts caused by excess protein.

the protein NOESY spectrum. The chemical shift changes caused by complexation are summarized in Table II and illustrated for the aromatic region in the contour plot of Figure 3. Binding of this tetranucleotide results in the marked upfield movement of cross peaks assigned to Tyr-26, Phe-73, and Leu-28. Cross peaks from Phe-13 and Tyr-34 shift slightly upfield, while those of Tyr-41 appear to move together somewhat, leading to partial overlap with the diagonal. Other aromatic spin systems and most of the protein resonances in crowded spectral regions show no significant movement ($\Delta\delta < 0.02$ ppm). The nucleotide-induced spectral changes observed in the NOESY spectrum are consistent with, and suggest a reinterpretation of, an earlier 1D difference spectrum [see Figure 2 of O'Connor and Coleman (1983)]. That 1D spectrum was originally interpreted as indicating that $d(pA)_4$ binding produced significant shifts of resonances from three Tyr residues (O'Connor & Coleman, 1983). However, the improved dispersion of the present NOESY spectra indicates that complexation causes major shifts of the resonances of only one Tyr residue. The above points out that a large degree of caution should be taken in the interpretation of 1D difference spectra in which several resonances have shifted by varying degrees, producing overlapped difference patterns. Further complications arise from the presence of complexation-induced resonance broadening, which may vary from one spin system to another.

Complexation with $d(pA)_4$ causes more line broadening than might be expected from a consideration of relative rotational correlation times (M_r 22 000 for the complex and 19 400 for free G5P). This suggests the formation of a small population of higher aggregation states, estimated to involve less than 5% of the protein. Such an estimate is in reasonable agreement with values derived from sedimentation experiments performed under somewhat different conditions (Pörschke & Rauh, 1983). A small temperature dependence is exhibited by the

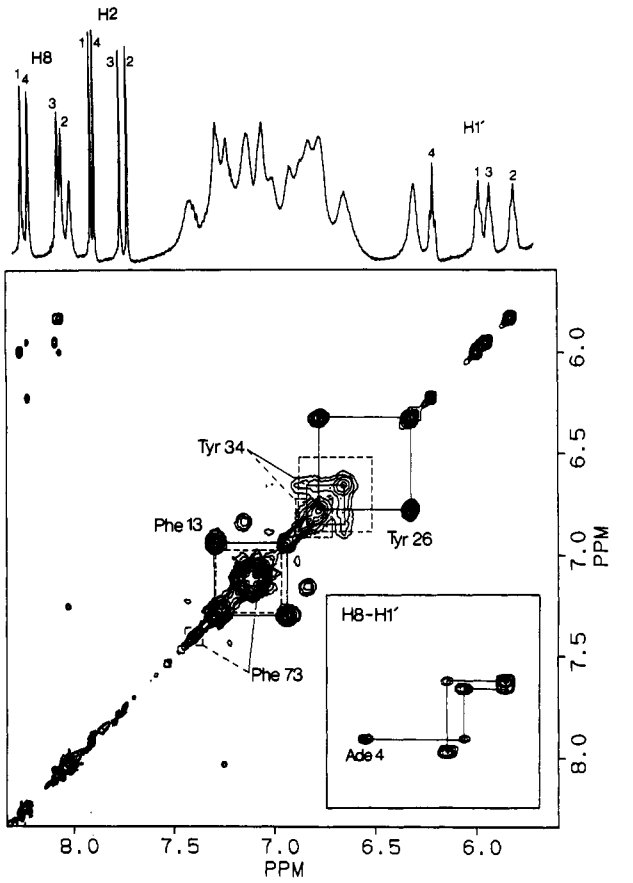

FIGURE 3: A 175-ms NOESY spectrum of a 1.5:1 mixture of $d(pA)_4$ and G5P, with 1D reference spectrum (conditions: 15 mM phosphate, 100 mM NaCl, pH 7.6, 35 °C). Several protein spin systems that shift upon complexation are indicated; dashed lines represent their original positions. (Inset) An expansion of sequential connectivities between the H8 and H1′ resonances of the nucleotide. Assignments for nucleotides 1–4 are indicated with the 1D spectrum.

Tyr-26 and Phe-73 resonances of the complex, which move approximately 0.05 ppm further upfield as the temperature is lowered to 15 °C.

Similar chemical shift effects are observed when $d(A)_4$ is the binding partner (Table II and Figure 4). Movements of the Tyr-26, Phe-73, and Leu-28 cross peaks are slightly smaller than those caused by $d(pA)_4$, reflecting the somewhat weaker binding and greater salt sensitivity conferred by the absence of a 5′-phosphate. Shifts of the Tyr-34, Phe-13, and Tyr-41 resonances are now close to zero. Even more clearly than observed in the case of $d(pA)_4$, it is apparent that only one tyrosine spin system (Tyr-26) is significantly affected by $d(A)_4$ binding.

As shown in the inset to Figure 3, NOEs between the H8 and H1′ resonances of $d(pA)_4$ can be used to make sequential assignments (Clore & Gronenborn, 1985; Scheek et al., 1983; Hare et al., 1983) with the knowledge that the lowest field H1′ resonance in an oligo(dA) spectrum derives from the 3′-terminal nucleotide residue (Olsthoorn et al., 1980). The H2 resonances of $d(pA)_4$ have been assigned with NOEs obtained from 1.0-s NOESY spectra, and their chemical shifts follow the pattern of the H8 resonances, as expected from the relative stacking of each nucleotide in the sequence. Two internucleotide H8–H1′ NOEs can be observed for $d(A)_4$ under the present conditions (Figure 4, inset), and data on lower homolgues reported by Oltshoorn et al. (1980) can be used to make the rest of the assignments (see Figure 4). It should be noted that while the sequential assignment process used here assumes a right-handed helical conformation for the

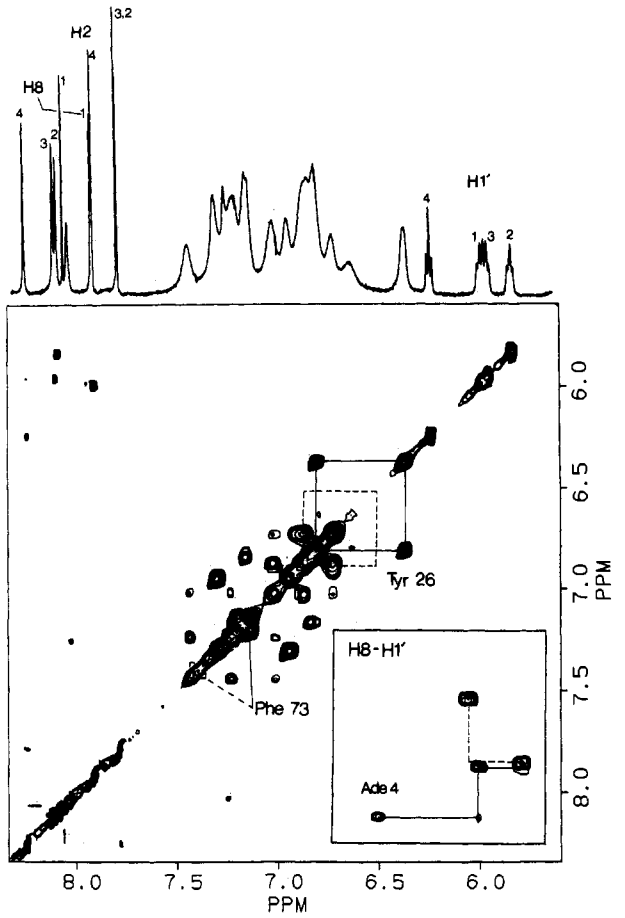

FIGURE 4: A 200-ms NOESY spectrum of a 1.1:1 mixture of $d(A)_4$ and G5P acquired under the conditions of Figure 3. (Inset) Sequential connectivities involving the nucleotide H8 and H1′ resonances, where the dotted connectivity has been inferred from other data (Olsthoorn et al., 1980).

nucleotide, such a conformation need not necessarily pertain to the "fully bound" species.[3]

Addition of excess protein to each tetranucleotide results in the nucleotide chemical shift changes that are summarized in Table II. Significant downfield shifts are observed for the Ade-2 and Ade-3 H2 resonances of $d(pA)_4$, while the H8 resonances shift upfield slightly and the H1′ signals show no common trend. Resonances of $d(A)_4$ generally shift to a lesser degree. Since the chemical shifts of other sugar resonances change by small amounts and interpretation of their shifts is problematic, no data are given for these resonances. Individual bases tend to maintain an anti conformation about the glycosidic bond, as indicated by the fact that the intensities of intranucleotide NOEs of the H8 resonances with sugar resonances follow the order H2′/H2″ > H1′, H3′ as shown in the example of Figure 5a. The sole exception is Ade-1 in $d(A)_4$, whose H8 resonance has a larger NOE with its H1′ (Figure 5b), indicating that the absence of a 5′-phosphate introduces a preference for the syn conformation.

Though the upfield chemical shift changes provide circumstantial evidence for nucleotide base–amino acid interactions, definitive proof of these interactions can best be obtained by the additional observation of intermolecular NOEs. Initially, attempts were made to observe G5P–tetranucleotide NOEs with 1D methods. These were not successful, due to a combination of signal-to-noise, irradiation spillover, and base line definition problems associated with our current instrumentation. Such problems were not unexpected, given the conditions that previous investigators found necessary for the observation of intermolecular NOEs in the $d(A)_8$–G5P complex (Alma et al., 1983). On further examination, we found that $d(pA)_4$–G5P NOEs could be repeatedly observed in NOESY spectra acquired with mixing times in the range of 0.75–1.0 s. At these long mixing times, signal-to-noise loss due to T_1 relaxation is potentially troublesome but can be partially offset by acquiring data over a relatively short t_1 period. Figure 6 shows NOEs observed between $d(pA)_4$ and G5P under low ionic strength conditions. Areas a–d contain cross peaks involving the following resonances: (a) Ade-2 H2–Phe-73 (3,5)/(4)H and (2,6)H and Ade-3 H2–Phe-73 (3,5)/(4)H and (2,6)H; (b) Ade-2 H8– and/or Ade-3 H8–Phe-73 (3,5)/(4)H and (2,6)H; (c) Ade-2 H1′–Phe-73 (2,6)H; (d) Ade-1 H1′–Tyr-26 (3,5)H. The intermolecular NOE cross peaks are rather small as expected, but are clearly evident above the local background. Relative intensities are difficult to reliably determine under these conditions, but it does appear that the cross peaks in area a are the most intense of the group, followed by those in area b. In the latter case, the precise identity of the nucleotide H8 resonance cannot be determined due to overlap of the Ade-2 and Ade-3 H8 signals, but the fact that both the Ade-2 and Ade-3 H2 resonances show NOEs with Phe-73 suggests that both H8 resonances may also show them. Similar experiments were not performed on $d(A)_4$–G5P mixtures, as the sharper nucleotide resonances caused greater t_1 noise problems.

At protein:nucleotide ratios near 1:1, some of the nucleotide base resonances from both tetranucleotides were observed to exhibit broadening and/or doubling behavior characteristic of chemical exchange processes, even though the protein resonances (including those markedly shifted by complexation) did not appear to deviate from classical fast-exchange behavior. These effects were not observed under all conditions of ionic strength and temperature, suggesting that a multistep exchange process exists which has relative rate constants such that individual spectral species can only be observed under favorable circumstances.

Complexation of G5P with $d(pT)_4$. In order to ensure that effects observed on complexation of $d(pA)_4$ and $d(A)_4$ were not simply a consequence of the helical conformations of these nucleotides, we investigated the interaction of G5P with $d(pT)_4$, which is considered to have a somewhat extended structure with no base stacking (Camerman et al., 1976; Saenger, 1983). As summarized in Table II, excess $d(pT)_4$ causes spectral changes very similar to those observed on complexation with the adenine-containing tetranucleotides. Specifically, the NOESY cross peaks of Tyr-26, Phe-73, and Leu-28 shift upfield to a greater extent than the others. The complexation-induced shifts are somewhat smaller, presumably due to the lesser ring current field of thymine (Giessner-Prettre & Pullman, 1976), but appear to be entirely analogous.

There appears to be a tighter base–aromatic interaction in this case, since the most upfield H6 resonance(s) of the nucleotide has (have) an NOE with the Phe-73 (3,5)H/(4)H

[3] Though correlation time considerations suggest that the observation of significant negative NOEs reflects *a* bound state of the nucleotide (Clore & Gronenborn, 1983), this state need only be one with a reasonable population that is in fast exchange with the free species. These conditions could be met by a nonspecifically bound species in the case of excess nucleotide or by an intermediate that lies between the free and fully bound states. Thus, the mere observation of NOEs suggesting a right-handed helix should not be overinterpreted in the absence of other data. This may have relevance to a recent study of *Escherichia coli* SSB protein (Clore et al., 1986), where such NOEs were used to conclude that aromatic amino acids did not intercalate between bases.

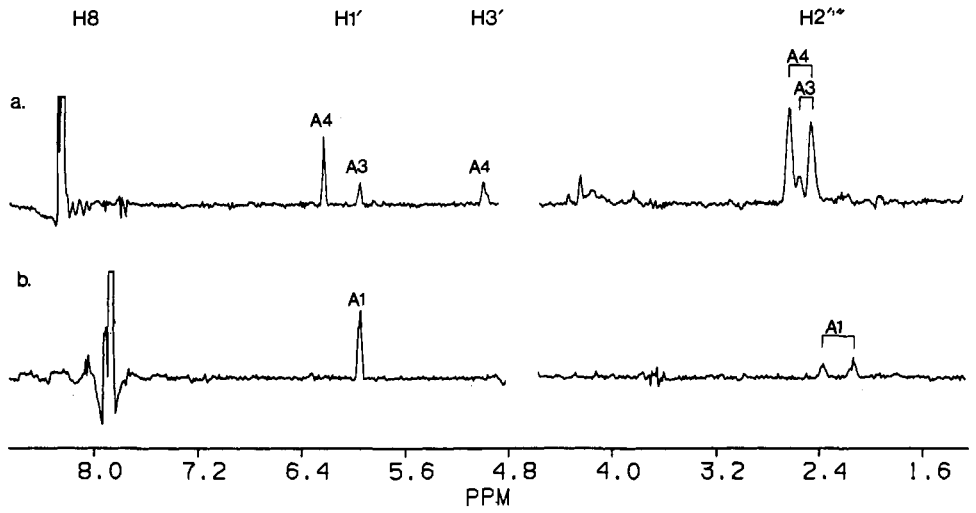

FIGURE 5: Representative NOESY cross sections involving nucleotide H8 diagonal peaks. (a) Section through the Ade-4 H8 diagonal from the NOESY spectrum of Figure 3. Intra- and internucleotide NOEs characteristic of anti and right-handled helical conformations are indicated. (b) Section through the Ade-1 H8 diagonal from the NOESY spectrum of Figure 4. Intranucleotide NOEs characteristic of a syn conformation are indicated.

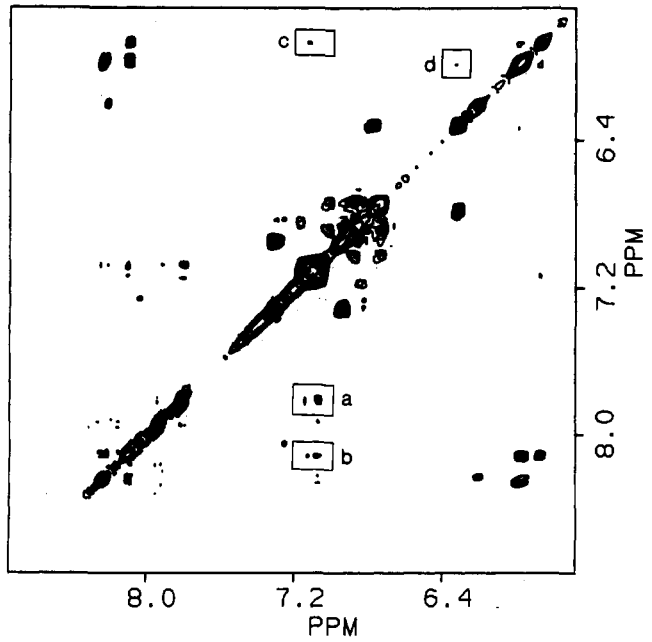

FIGURE 6: Aromatic region from an 800-ms NOESY spectrum of a 1:1 $d(pA)_4$–G5P mixture (conditions: 10 mM phosphate, 25 mM NaCl, pH 7.6, 35 °C). Protein–nucleotide NOEs are indicated in areas a–d.

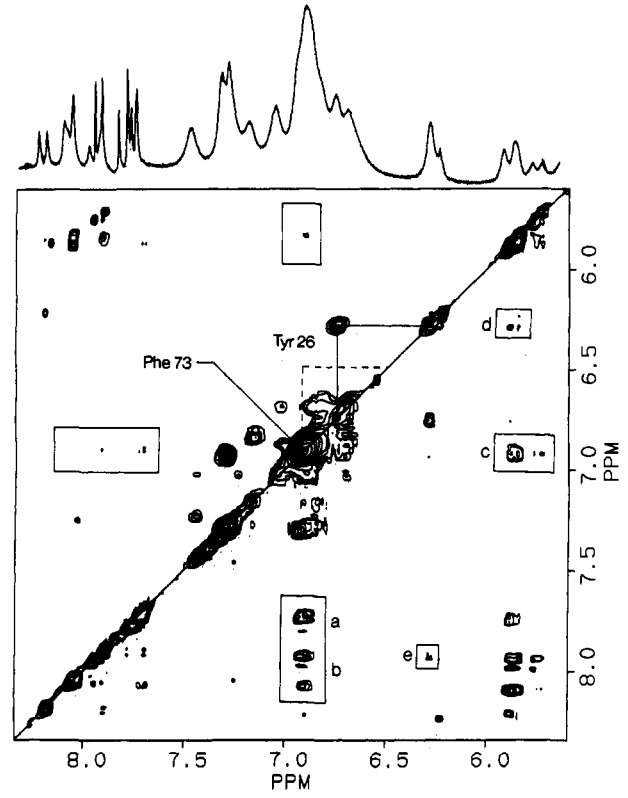

FIGURE 7: Combined aromatic regions from a 200-ms NOESY spectrum (upper triangle) and a 750-ms NOESY spectrum (lower triangle) of a 0.5:1 $d(pA)_8$–G5P mixture, with 1D reference spectrum (conditions: 20 mM phosphate, 125 mM NaCl, pH 7.6, 35 °C). Intermolecular NOEs obtained at a 750-ms mixing time are indicated in areas a–e, designated to show their correspondence with the NOEs of Figure 6. Some of these NOEs are just evident in the 200-ms spectrum.

resonance, which has a significant intensity at a mixing time of 250 ms. Unfortunately, two H6 resonances overlap at this position and the nonstacked conformation of the oligonucleotide precludes sequential assignments, since no internucleotide H6–H1′ NOEs are observed. However, a consideration of end effects suggests that the signal responsible for the protein–nucleotide NOE arises from the Thy-2 and/or Thy-3 H6 group.

Complexation of G5P with $d(pA)_8$. Since the binding site of G5P is four nucleotides long, complexation with an octanucleotide forms a cooperatively bound species of M_r 44 000. In practice, this species is in equilibrium with partially bound and free forms but is expected to predominate under suitable conditions. Addition of $d(pA)_8$ to G5P in a 0.5:1 ratio results in protein resonance shift changes similar in nature to those caused by the tetranucleotides under similar conditions, but which tend to be larger (Figure 7 and Table II). Tyr-26 and Leu-28 NOESY cross peaks move upfield to a somewhat greater extent, while the upfield shift of the Phe-73 resonances is close to doubled. Again, small movements are observed for the Tyr-34 and Phe-13 signals, while the precise effects on Tyr-41 cannot be detected because its cross peaks are obscured by overlap with the diagonal or other cross peaks. However, any movements of this spin system must be relatively small.

The H8 resonances of $d(pA)_8$ tend to manifest only intranucleotide NOEs with the H1′ signals (Figure 7); most of the signals do not appear to generate significant internucleotide

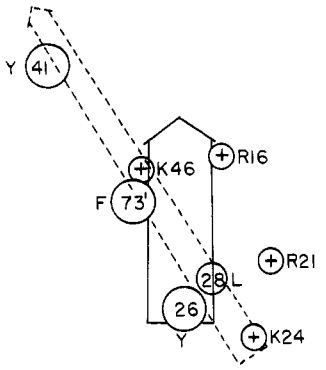

FIGURE 8: Schematic comparison of the G5P–oligonucleotide interaction suggested by this work with that proposed by Brayer and McPherson (1984). The solid arrow indicates an approximate nucleotide path dictated by the electropositive groups of Arg-16, Arg-21, Lys-24, and Lys-46. As suggested by the NMR data, Tyr-26, Leu-28, and Phe-73′ lie in positions to stack with nucleotide bases. The dashed arrow (thinner and longer to imply complete unstacking of five nucleotides) depicts the path predicted by Brayer and McPherson.

NOEs, even at a mixing time of 750 ms. This prevents the direct use of sequential assignments but does suggest that the helical conformation of the nucleotide is significantly perturbed in the complex.

As a consequence of the relatively tight binding displayed by $d(pA)_8$ (Coleman et al., 1976), specific protein–nucleotide NOEs can be observed at mixing times of 100–200 ms, several of which become quite intense at a mixing time of 750 ms (Figure 7). As indicated by the designations of areas a–e in Figure 7, the pattern of intermolecular NOEs exhibited by $d(pA)_8$ closely resembles that observed for the $d(pA)_4$–G5P complex. This suggests that the tetra- and octanucleotides interact in a similar manner. Resonance overlap and the lack of specific assignments make it difficult to interpret the $d(pA)_8$–G5P NOEs unequivocally in terms of specific nucleotide–aromatic interactions. However, it is clear that intermolecular NOEs only involve the Phe-73 and Tyr-26 resonances. Of four intense NOEs with the Phe-73 resonances in areas a and b, two involve Ade H2 signals, one involves an H8 resonance, and one may derive from either an H8 or H2 signal (Figure 7).

Structure of the G5P–Oligodeoxynucleotide Complex. The NMR data presented in this paper place a number of restrictions on any model of the G5P–oligonucleotide interaction. From the general observation of complexation-induced upfield shifts on the resonances of Tyr-26, Leu-28, and Phe-73, it can be concluded that these residues form a dominant interaction site that is involved in stacking interactions with nucleotide bases. The observation of intermolecular NOEs between the protons of Tyr-26 and Phe-73 and the H8 and H2 protons of Ade rings (Figures 6 and 7) strengthens this proposal. Conversely, the absence of significant chemical shift effects of intermolecular NOEs involving the protons of Tyr-34 and Tyr-41 suggests that these two aromatics do not interact with the bases of an oligodeoxynucleotide.

The above conclusions are at variance with a model of the G5P–nucleic acid interaction that has been proposed on the basis of manual model building on the unliganded protein with reference to previous spectroscopic and chemical modification data (Brayer & McPherson, 1984). In particular, that model predicts stacking of nucleotide bases on Tyr-34 and Tyr-41, for which we have found no evidence in our NOESY spectra. Figure 8 shows a schematic structure for the G5P–oligonucleotide complex that better fits our observations, compared with a similar depiction of the Brayer–McPherson model. Computer-graphic examination of the G5P X-ray structure reveals that Tyr-26, Leu-28, and Phe-73′[2] are located in the region of an electropositive cluster formed by the side chains of Arg-16, Arg-21, Lys-24, and Lys-46. Tyr-26 and Phe-73′ can be viewed as the jaws of a "clamp", backed by Leu-28, which encloses nucleotide bases. While NOESY data indicate that the clamp encloses two bases in the case of $d(pA)_4$, only one base may be enclosed in other nucleotides. The precise role of Leu-28 is unclear at present, as no definitive protein–nucleotide NOEs have been observed for this residue.

Electrostatics are expected to dominate the protein–oligonucleotide interaction, leading to a nucleotide path that passes through the center of the positively charged patch, as depicted by the solid arrow in Figure 8. While the observed ring current shifts and the intermolecular NOEs place an upper limit of approximately 4 Å on the distance between the individual Ade rings and the Tyr-26–Phe-73′ clamp, these data alone do not allow detailed model building. Three of four Ade rings approach Tyr-26 and Phe-73′. In contrast, the Brayer–McPherson model directs a fifth and final nucleotide over to stack on Tyr-41, a path indicatd by the dashed arrow. We believe this path to be unlikely on the basis of our NMR data and the generally accepted view that the binding stoichiometry of G5P is four or less nucleotides per monomer, depending on the conditions (Alma et al., 1983a; Bulsink et al., 1986; Kansy et al., 1986).

There are more subtle disagreements between the two models, one of which is related to the difference in nucleotide path lengths. Our chemical shift data for the adenylyl nucleotides suggests that only partial base unstacking occurs on complexation, rather than the complete unstacking proposed by Brayer and McPherson. In addition, the present model does not use Arg-80 in a phosphate-binding role as this residue is salt-bridged with Glu-30 in the X-ray structure, while the Brayer–McPherson model postulates a breakage of this bridge on nucleotide binding.

NMR data suggest the presence of considerable motional freedom or multiple conformational equilibria within the G5P–oligonucleotide complex. These processes are presumably responsible for the fact that relatively long mixing times are necessary to observe intense intermolecular NOEs. In the interests of brevity, we have not made detailed comparisons between the 2D NOESY results and previous NMR studies of G5P–oligodeoxynucleotide interactions. These will be covered elsewhere, as will more detailed model building, assigning the relative proximities of the sugar as well as the base protons to the aromatic rings.

The validity of extrapolating the details of the present model to the structure of the in vivo G5P–fd DNA superhelix is unclear, since there have been suggestions that G5P may bind to oligo- and polynucleotides in different ways (Alma et al., 1982; Kansy et al., 1986). However, it is apparent that a nucleotide path of the type proposed here may facilitate "inside" packing of DNA, a topology suggested by neutron scattering results (Gray, D. M., et al., 1982) but one incompatible with a structure proposed from modeling (Brayer & McPherson, 1985; McPherson & Brayer, 1985).

ACKNOWLEDGMENTS

We thank Dr. Richard Prigodich for the gift of dTyr, Dr. Jim Warwicker for his assistance with the Evans and Sutherland system, and Dr. James Prestegard for providing access to the AMBER package.

Registry No. Phenylalanine, 63-91-2; tyrosine, 60-18-4; leucine, 61-90-5.

References

Alberts, B. M., Frey, L., & Delius, H. (1972) *J. Mol. Biol. 68*, 139–152.

Alma, N. C. M., Harmsen, B. J. M., Hilbers, C. W., van der Marel, G. & van Boom, J. H. (1981a) *FEBS Lett. 135*, 15–20.

Alma, N. C. M., Harmsen, B. J. M., Hull, W. E., van der Marel, G., van Boom, J. H., & Hilbers, C. W. (1981b) *Biochemistry 20*, 4419–4428.

Alma, N. C. M., Harmsen, B. J. M., van Boom, J. H., van der Marel, G., & Hilbers, C. W. (1982) *Eur. J. Biochem. 122*, 319–326.

Alma, N. C. M., Harmsen, B. J. M., deJong, E. A. M., van der Ven, J., & Hilbers, C. W. (1983a) *J. Mol. Biol. 163*, 47–62.

Alma, N. C. M., Harmsen, B. J. M., van Boom, J. H., van der Marel, G., & Hilbers, C. W. (1983b) *Biochemistry 22*, 2104–2115.

Anderson, R. A., Nakashima, Y., & Coleman, J. E. (1975) *Biochemistry 14*, 907–917.

Baumann, R., Wider, G., Ernst, R. R., & Wüthrich, K. (1981) *J. Magn. Reson. 44*, 402–406.

Brayer, G. D., & McPherson, A. (1983) *J. Mol. Biol. 169*, 565–596.

Brayer, G. D., & McPherson, A. (1984) *Biochemistry 23*, 340–349.

Brayer, G. D., & McPherson, A. (1985) *Eur. J. Biochem. 150*, 287–296.

Bulsink, H., van Resandt, R. W. W., Harmsen, B. J. M., & Hilbers, C. W. (1986) *Eur. J. Biochem. 157*, 329–334.

Bundi, A., & Wüthrich, K. (1979) *Biopolymers 18*, 285–297.

Camerman, N., Fawcett, J. K., & Camerman, A. (1976) *J. Mol. Biol. 107*, 601–621.

Campbell, I. D., Dobson, C. M., Williams, R. J. P., & Wright, P. E. (1975) *FEBS Lett. 57*, 96–99.

Cavalieri, S. J., Neet, K. E., & Goldthwait, D. A. (1976) *J. Mol. Biol. 102*, 697–711.

Clore, G. M., & Gronenborn, A. M. (1983) *J. Magn. Reson. 53*, 423–442.

Clore, G. M., & Gronenborn, A. M. (1985) *FEBS Lett. 179*, 187–198.

Clore, G. M., Gronenborn, A. M., Greipel, J., & Maas, G. (1986) *J. Mol. Biol. 187*, 119–124.

Coleman, J. E., & Armitage, I. M. (1977) in *NMR in Biology* (Dwek, R. A., Campbell, I. D., Richards, R. E., & Williams, R. J. P., Eds.) pp 171–200, Academic, New York.

Coleman, J. E., & Armitage, I. M. (1978) *Biochemistry 17*, 5038–5045.

Coleman, J. E., & Oakley, J. L. (1980) *CRC Crit. Rev. Biochem. 7*, 247–289.

Coleman, J. E., Anderson, R. E., Ratcliffe, R. G., & Armitage, I. M. (1976) *Biochemistry 15*, 5419–5430.

Cuypers, T., van der Ouderaa, F. J., & deJong, W. W. (1974) *Biochem. Biophys. Res. Commun. 59*, 557–563.

Day, L. A. (1973) *Biochemistry 12*, 5329–5339.

Garssen, G. J., Hilbers, C. W., Schoenmakers, J. G. G., & van Boom, J. H. (1977) *Eur. J. Biochem. 81*, 453–463.

Garssen, G. J., Kaptein, R., Shoenmakers, J. G. G., & Hilbers, C. W. (1978) *Proc. Natl. Acad. Sci. U.S.A. 75*, 5281–5285.

Garssen, G. J., Tesser, G. I., Schoenmakers, J. G. G., & Hilbers, C. W. (1980) *Biochim. Biophys. Acta 607*, 361–371.

Giessner-Prettre, C., & Pullman, B. (1976) *Biochem. Biophys. Res. Commun. 70*, 578–581.

Giessner-Prettre, C., Pullman, B., Borer, P. N., Kan, L.-S., & T'so, P. O. P. (1976) *Biopolymers 15*, 2277–2286.

Gray, C. W., Kneale, G. G., Lenard, K. R., Siegrist, H., & Marvin, D. A. (1982) *Virology 116*, 40–51.

Gray, D. M., Gray, C. W., & Carlson, R. D. (1982) *Biochemistry 21*, 2702–2713.

Hare, D. R., Wemmer, D. E., Chou, S. H., Drobny, G., & Reid, B. R. (1983) *J. Mol. Biol. 171*, 319–336.

Jones, A. T. (1978) *J. Appl. Crystallogr. 11*, 268–272.

Kansy, J. W., Clack, B. A., & Gray, D. M. (1986) *J. Biomol. Struct. Dyn. 3*, 1079–1110.

King, G. C., & Wright, P. E. (1986) *Biochemistry 25*, 2364–2374.

Klevit, R. E. (1985) *J. Magn. Reson. 62*, 551–555.

Kornberg, A. (1980) *DNA Replication*, pp 379–496, W. H. Freeman, San Francisco.

Kornberg, A. (1982) *Supplement to DNA Replication*, p 571, W. H. Freeman, San Francisco.

McPherson, A., & Brayer, G. D. (1985) in *Biological Macromolecules and Assemblies* (McPherson, A., & Jurnak, F., Eds.) Vol. 2, pp 323–392, Wiley, New York.

McPherson, A., Jurnak, F. A., Wang, A. H., Molineux, I., & Rich, A. (1979) *J. Mol. Biol. 134*, 379–400.

McPherson, A., Koszelak, S., Axelrod, H., Day, J., Williams, R., Robinson, L., McGrath, M., & Cascio, D. (1986) *J. Biol. Chem. 261*, 1969–1975.

Nakashima, Y., Dunker, A. K., Marvin, D. A., & Konigsberg, W. (1974) *FEBS Lett. 43*, 125.

O'Connor, T. P., & Coleman, J. E. (1982) *Biochemistry 21*, 848–854.

O'Connor, T. P., & Coleman, J. E. (1983) *Biochemistry 22*, 3375–3381.

Oey, J. L., & Knippers, R. (1972) *J. Mol. Biol. 68*, 125–138.

Olsthoorn, C. S. M., Bostelaar, L. J., van Boom, J. H., & Altona, C. (1980) *Eur. J. Biochem. 112*, 95–110.

Perkins, S. J. (1980) *J. Magn. Reson. 38*, 297–312.

Pörschke, D., & Rauh, H. (1983) *Biochemistry 22*, 4737–4745.

Pratt, D., Laws, P., & Griffith, J. (1974) *J. Mol. Biol. 82*, 425–439.

Pretorius, H. T., Klein, M., & Day, L. A. (1975) *J. Biol. Chem. 250*, 9262–9269.

Prigodich, R. V., Shamoo, Y., Williams, K. R., Chase, J. W., Konigsberg, W. H., & Coleman, J. E. (1986) *Biochemistry 25*, 3666–3672.

Saenger, W. (1983) *Principles of Nucleic Acid Structure*, Springer-Verlag, New York.

Scheek, R. M., Russo, N., Boelens, R., & Kaptein, R. (1983) *J. Am. Chem. Soc. 105*, 2914–2916.

States, D. J., Haberkorn, R. A., & Ruben, D. J. (1982) *J. Magn. Reson. 48*, 286–292.

Weiner, S. J., Kollman, P. A., Case, D. A., Singh, U. C., Ghio, C., Alagona, G., Profeta, S., & Weiner, P. (1984) *J. Am. Chem. Soc. 106*, 765–784.